

proposed mechanisms for the production of Schottky defects may equally well predominate.

CONCLUSIONS

The two principal experimental observations reported in this paper suggest that the formation of F centers at liquid helium temperature occurs as the result of the ejection of a halide ion (or atom) into the interstices of the lattice, leaving a vacancy which subsequently traps an electron and becomes an F center. These observations are as follows: first, F center formation at liquid helium temperature appears to be essentially a bulk property of the alkali halide, independent of both the defect structure and the

coloration at room temperature; and second, the energy required to form an F center at liquid helium temperature for various alkali halides is in agreement with the interstitial space available to accept the ejected halide ion (or atom). The suggestion of Känzig and Woodruff that the formation of F centers and H centers at liquid helium temperature is a paired process is in accord with these observations.

A comparison of the energy necessary to produce F centers at room temperature and low temperature lends additional support to the view that room temperature coloration occurs in two stages: the first consists of filling existing vacancies with electrons; in the second stage vacancies must be created.

Pressure Effects of Helium and Argon on the First Sharp Series Doublet of Indium*

SHANG-YI CH'EN, ALLEN SMITH, AND MAKOTO TAKEO
University of Oregon, Eugene, Oregon

(Received February 19, 1959; revised manuscript received August 3, 1959)

The shift, half-width, and asymmetry of the $\text{In}\lambda 4101$ and $\lambda 4511$ lines produced by various pressures of helium and argon up to 120 atmospheres and the appearance of satellite bands near these lines are described. The entire absorption line contours and the wings of the pressure-broadened lines were studied. The experimental observations were compared with the Anderson-Talman theory at general pressures.

I. INTRODUCTION

IN contrast to the much studied pressure broadening and shift of alkali doublets¹ with 2S as ground state, the corresponding study of the first sharp series doublet ($5^2P_{1/2}-6^2S_{1/2}$, $5^2P_{3/2}-6^2S_{1/2}$) of In ($\lambda 4101$ and $\lambda 4511$) facilitates the investigation of the perturbation of energy levels whose fine structure separation is due to the ground states 2P . The line contours, the shifts, and the satellites of these lines were observed for pressures up to 120 atmospheres of He and Ar by means of a 35-foot grating in Wadsworth mounting. For helium, the temperature of the absorption tube ranged from 800°C–1000°C for both lines, and for argon the temperature was constantly 800°C for $\lambda 4101$ and 900°C for $\lambda 4511$.

II. RESULTS

The speed of the grating spectrograph was $f/35$, and the plate constants for the $\lambda 4101$ and $\lambda 4511$ regions were 1.55 and 1.53 Å/mm, respectively. The slit width was 30 μ . Two different lengths of absorption column were used, 4.4 and 4.95 cm. Kodak type 103-0 plates were calibrated by means of step filters, and the line contours were analyzed with a recording microphotometer. During the course of this research great care was taken in designing the absorption tube to keep the

temperature of the absorption column uniform and constant. The accuracy of relative density values of foreign gases should be within 2%.

1. The Shift

Figure 1 is a plot of the observed values of shift $\Delta\nu_m$, in cm^{-1} , vs the relative density (r.d.) of argon or helium. For argon the *red* shift of the $\lambda 4101$ ($^2P_{1/2}$) component is practically the same as that of the $\lambda 4511$ ($^2P_{3/2}$) component. For He the *violet* shift of the $\lambda 4101$ component is slightly smaller than that of the $\lambda 4511$ component. The magnitude of the red shift produced by argon is about three times greater than the violet shift produced by helium. Empirical equations which describe the present data are:

For In 4101/argon:

$$-\Delta\nu_m = 0.408(\text{r.d.}) + 0.012(\text{r.d.})^2 \text{ cm}^{-1}. \quad (1)$$

For In 4511/argon:

$$-\Delta\nu_m = 0.454(\text{r.d.}) + 0.0095(\text{r.d.})^2 \text{ cm}^{-1}.$$

For helium as a perturber we can obtain a relation similar to Eq. (1), but the error appearing in the second term would be very large. A theoretical equation for the line shift is given in Part III.

* Sponsored by the Office of Ordnance Research, U. S. Army.
¹ S. Y. Ch'en and M. Takeo, *Revs. Modern Phys.* **29**, 20 (1957).

2. The Broadening and Asymmetry

The half-width of the two doublet components *vs* r.d. of argon or helium shows (Fig. 2) that there is a linear relationship between the half-width and the r.d. of foreign gases. The slopes (in $\text{cm}^{-1}/\text{r.d.}$) of the curves for helium are 1.13 and 1.18 for the $^2P_{1/2}$ and $^2P_{3/2}$ components, respectively. The corresponding values for argon are, respectively, 1.23 and 1.10. It appears that for argon the relative broadening of the fine structure components for the sharp series doublet of indium is just the reverse of the case for the principal series doublets of alkalis.

The asymmetries of the lines were measured by the ratios of the red half to the violet half of the half-width. Thus red asymmetries will be indicated by numbers

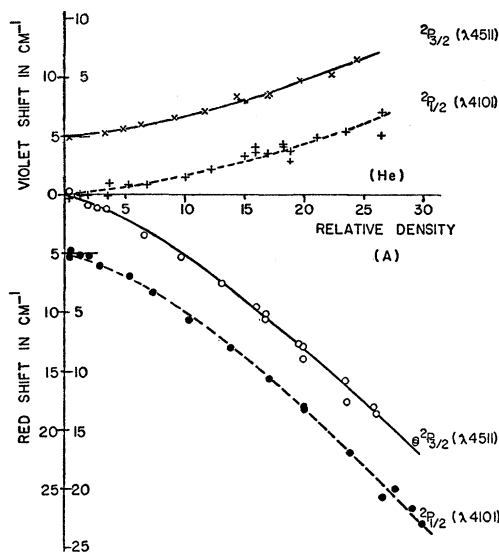


FIG. 1. The shift of the first sharp series doublet lines of indium for various relative densities of helium and argon.

greater than 1 and violet asymmetries by numbers less than 1. The precision of the asymmetry measurements was limited when the r.d. was low because the lines were very narrow and the half-width determination was inaccurate, and also when the r.d. was too high because it was difficult to determine the intensity maxima of highly broadened lines.

The red asymmetry of lines produced by argon increases steadily from 1 to about 1.9 as the r.d. increases from 0 to 10, levels off between r.d. 10 to 20, and then falls off to about 1.5 at r.d. 30. The violet asymmetry of lines produced by helium increases monotonically from 1 at very low r.d. to 0.7 at r.d. 30. This is shown in Fig. 3.

3. The Violet Satellite Band

Figure 4 is a microphotometer curve showing the violet satellite of In4101 observed at 798°C with 110.3

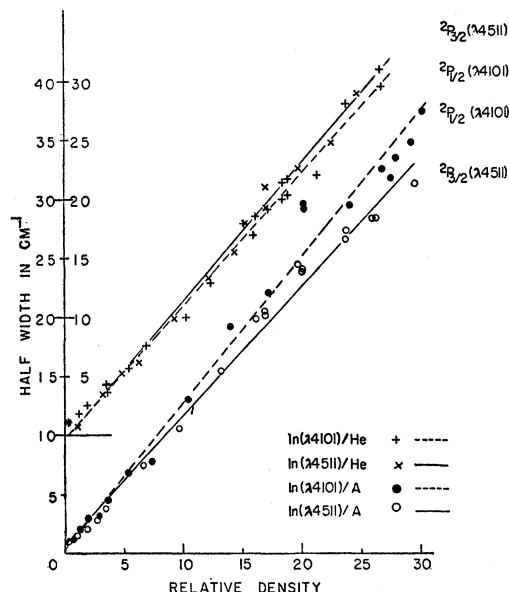


FIG. 2. The broadening of the first sharp series doublet lines of indium for various relative densities of helium and argon.

atmos of argon. The frequency of the satellite maximum was 69 cm^{-1} higher than that of the perturbed $\lambda 4101$ (at 24353 cm^{-1}). The (satellite/ $\lambda 4101$ line) spectral intensity ratio was 0.049. The length of absorption column was 4.95 cm, and $\alpha_{\text{band}} = 0.074$, $\alpha_{\text{line}} = 0.682$, where α_{band} and α_{line} are the absorption coefficients per cm of the band and the line at their maxima, respectively. From an integration of the area of the absorption contour, the total intensity of the satellite is 0.19 of that for the entire line. The half-width of the satellite was 67 cm^{-1} while that of the broadened line was 32 cm^{-1} . There was an indication, also, of a violet band for $\lambda 4511$. Under the conditions of the experiment it was not feasible to make accurate measurement of its intensity maximum.

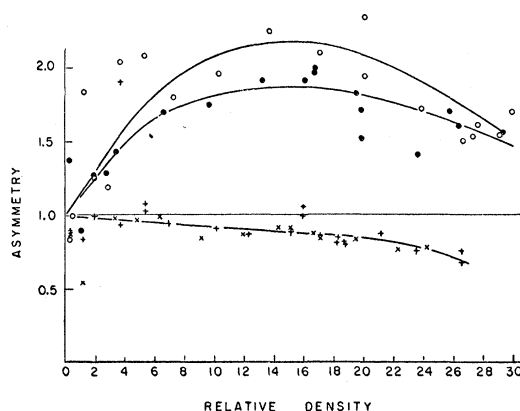


FIG. 3. The asymmetry of In4101 and In4511 broadened by argon and helium. The data for In4101/argon and In4511/argon were denoted by \circ and \bullet respectively; for In4101/He and In4511/He, by $+$ and \times .

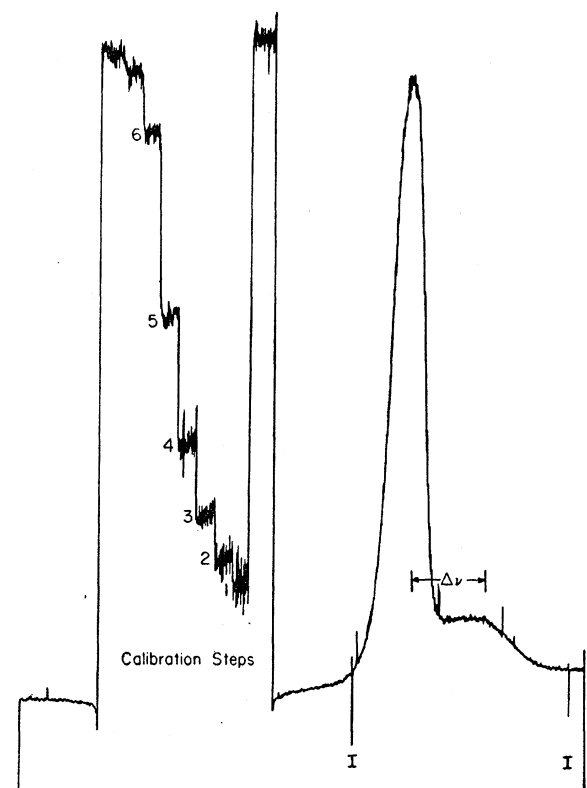


FIG. 4. Microphotometer trace of the violet satellite of In4101 in the presence of argon (110.3 atmospheres, 798°C).

4. Pressure Broadened Line Contours

(a) The Wings

To study the intensity distribution of the wings of the lines, D and $\Delta\nu$ were plotted logarithmically (see Fig. 5), D being the density of the absorption line at a frequency which was higher than that of the unshifted line maximum by $\Delta\nu$. Theoretically the red wing of the lines broadened by argon should fall off as $\Delta\nu^{-(1+3/p)}$ or $\Delta\nu^{-3/2}$ for the interaction of the form γ/r^6 , as first pointed out by Kuhn.² The violet wing is expected to follow Lindholm's $\Delta\nu^{-7/3}$,³ or Anderson-Talman's exponential form.⁴

As shown in Fig. 6 our experimental results for In4511 showed that the red wing followed closely the $\Delta\nu^{-3/2}$ law for r.d. of argon ranging from 3 to 6. The line for Curve A was rather narrow (see Fig. 6) so that only for $\Delta\nu$ from 1 to $3\frac{1}{2}$ times $\Delta\nu_{1/4}$, the contour followed the $-3/2$ power relationship. ($\Delta\nu_{1/4}$ denotes the half of the half-width.) Curve B indicates that the wing followed closely the $-3/2$ power relationship for a range of $\Delta\nu$ from 2 to 10 cm^{-1} (equivalent to 1.5 to 7 times $\Delta\nu_{1/4}$). The corresponding range of $\Delta\nu$ for Curve C was

² H. Kuhn, Proc. Roy. Soc. (London) **A158**, 212 (1937).

³ E. Lindholm, Arkiv. Mat. Astron. Fysik **32A**, No. 17 (1945).

⁴ P. W. Anderson and J. D. Talman, Proceedings on the Conference on Broadening of Spectral Lines, p. 29 (1956), or Eq. (130) of footnote 1.

from 9 to 20 cm^{-1} or 2 to 5 times $\Delta\nu_{1/4}$. For r.d. much higher than 6 the intensity distribution showed a continuously increasing slope with no specific indication of a range for the $-3/2$ power law. The portion of the red wing which followed Kuhn's $-3/2$ power law is marked by a bold line in Fig. 6. This same behavior was observed also for In4101/A.

Note also that there is nothing anomalous about Curve E (in Fig. 5) although the r.d. for this case lay

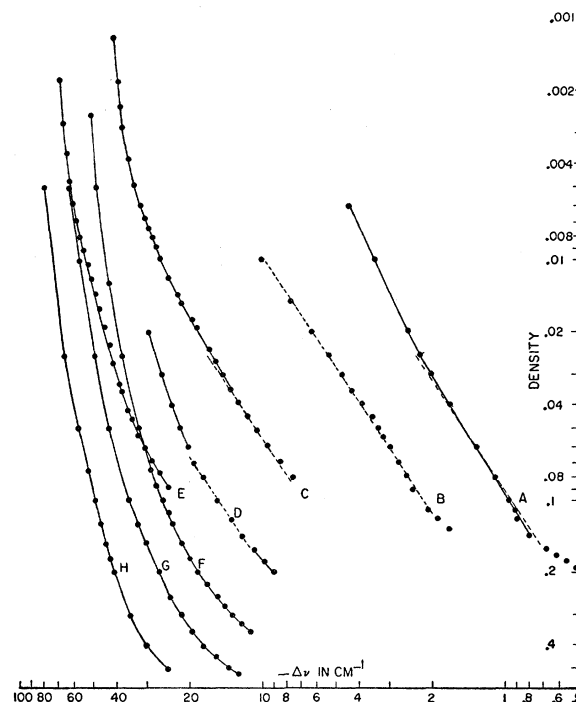


FIG. 5. Plot of $\log D$ vs $\log \Delta\nu$ for the red wing of In4511 under various r.d. of argon. Captions to various curves are given in the appended table, and apply also to Figs. 6 and 7.

Curve	r.d.	Temp.	Curve	r.d.	Temp.
A	1.02	1121°K	E	19.92	1107°K
B	2.71	1126°K	F	13.12	1132°K
C	6.63	1119°K	G	16.03	1137°K
D	9.69	1127°K	H	21.12	1131°K

For comparison, dashed straight lines were drawn with a slope of $-\frac{3}{2}$.

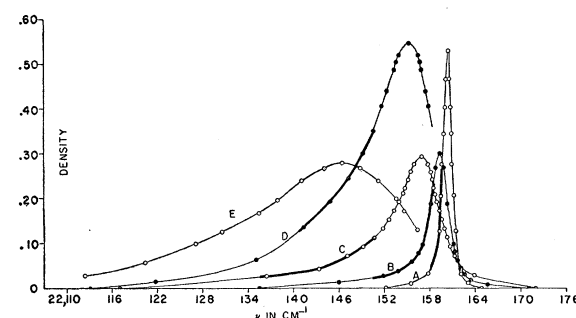
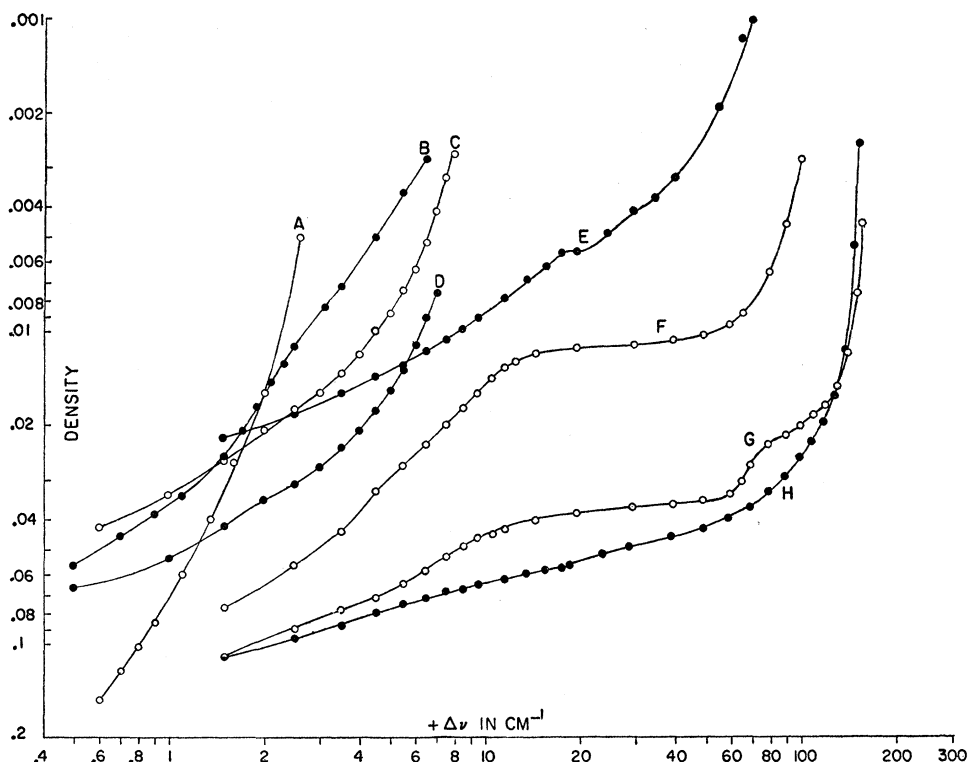


FIG. 6. The line contours of the In4511 line broadened by argon. The part of the red wing which follows closely Kuhn's $-\frac{3}{2}$ power law is lined more heavily.

FIG. 7. Plot of $\log D$ vs $\log \Delta\nu$ for the violet wing of In4511 for various relative densities of argon.



between those for curves *G* and *H*; the line was much fainter because of a lower temperature of the absorption column.

Figure 7 shows the corresponding data for the violet wing of the lines. There is no clear indication that there is a simple relationship to describe the wing distribution. The irregularities of the curves were more pronounced for higher r.d. and were chiefly due to the superposition of the line and the diffused satellite. The curves are less distorted if the intensity of the satellite is suppressed by lowering the temperature, as shown in Curve *E*.

Similar plots were also made for both In4511 and 4101 with various helium pressures. For the red wings, the intensity increased in a nonlinear fashion as Curves *E* to *H* in Fig. 5. For the violet wings, a considerable portion of each of the curves was linear, but the slopes seemed to vary continuously from 1.6 to 1.4 over the observed r.d. ranges: 1 to 28.

(b) The Center Part of the Line Contours

Figures 8 (a)-(d) show some line contours of In4101 and In4511 broadened by argon, and Fig. 8 (e) is a

typical intensity distribution of In4511 broadened by helium. The solid line and the circles indicate the experimental observations. The dotted and dashed curves are the results of theoretical calculations which will be detailed in the next section.

III. DISCUSSION

A. Pressure Effects of Argon on In4101 and In4511

The above-discussed shape of the red wing seems to indicate that the line shape would agree with the classical statistical broadening theory, although the situation for the violet wing is quite different. The violet wing is modified by the superposition of the line and the satellite. This is due to nonadiabatic collisions, since the adiabatic collisions are supposed to affect both wings to nearly the same extent.

For low relative density and small $\Delta\nu$, the classical theoretical intensity distribution of a pressure-broadened line under an angular frequency perturbation of the line, $\Delta\omega = -\gamma/r^p$, has been given by many people and recently by Anderson-Talman.⁴

$$I(\Delta\omega') = e^{-1.91h} \frac{\sigma_0 h \cos(\pi/p-1) \cos 2.63h - \sin 2.63h [\Delta\omega' + \sigma_0 h \sin(\pi/p-1)]}{[\Delta\omega' + \sigma_0 h \sin(\pi/p-1)]^2 + [\sigma_0 h \cos(\pi/p-1)]^2}, \quad (2)$$

where

$$h = NR_0^3, \quad R_0 = \left(\frac{\gamma}{v}\right)^{1/p-1}, \quad \Delta\omega' = \frac{R_0}{v} \Delta\omega, \quad \sigma_0 = \pi \left(2 \int_0^\infty \frac{du}{(1+u^2)^{p/2}}\right)^{2/p-1} \Gamma\left(1 - \frac{2}{p-1}\right),$$

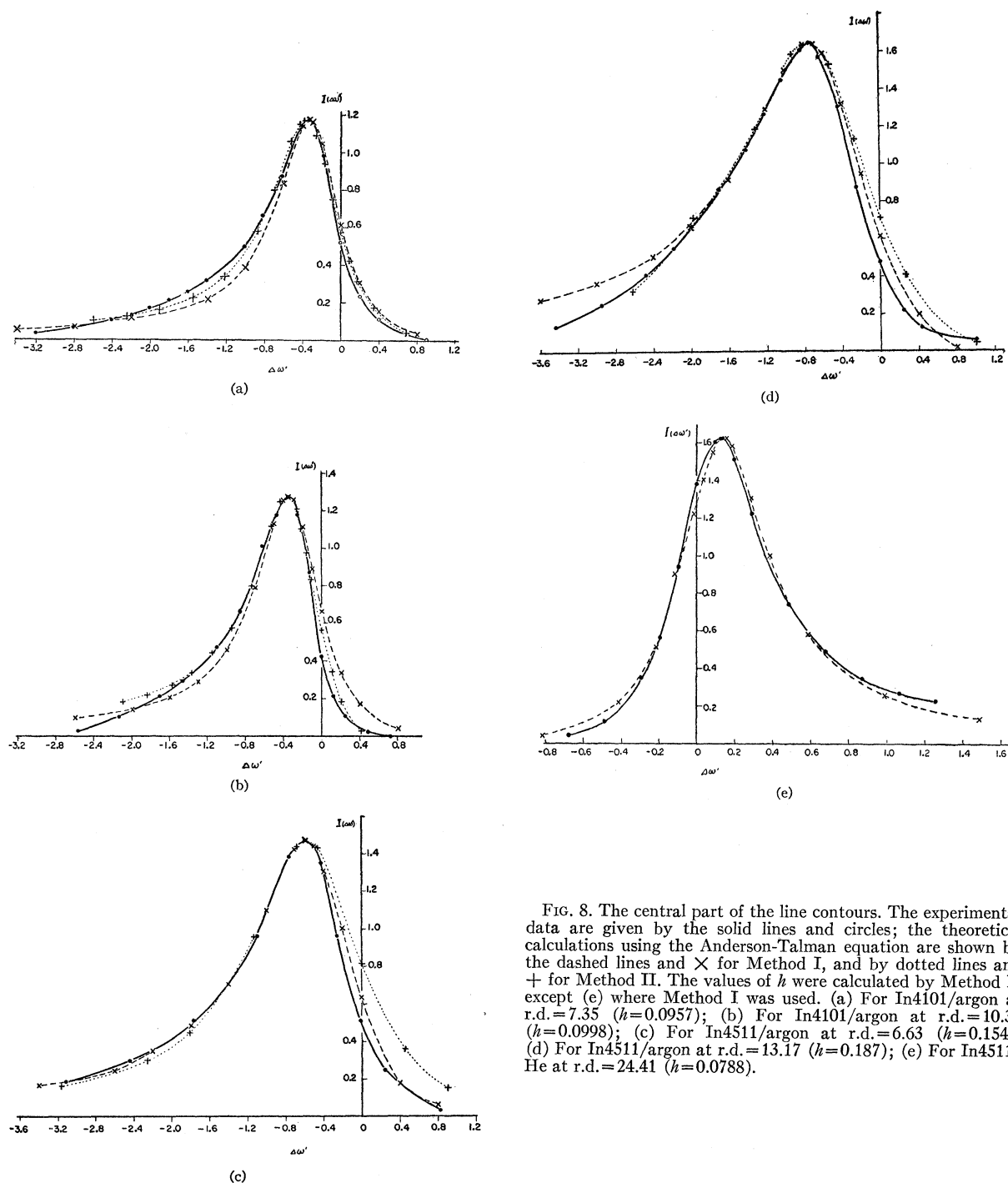


FIG. 8. The central part of the line contours. The experimental data are given by the solid lines and circles; the theoretical calculations using the Anderson-Talman equation are shown by the dashed lines and \times for Method I, and by dotted lines and $+$ for Method II. The values of h were calculated by Method II except (e) where Method I was used. (a) For In4101/argon at r.d.=7.35 ($h=0.0957$); (b) For In4101/argon at r.d.=10.36 ($h=0.0998$); (c) For In4511/argon at r.d.=6.63 ($h=0.154$); (d) For In4511/argon at r.d.=13.17 ($h=0.187$); (e) For In4511/He at r.d.=24.41 ($h=0.0788$).

v is the mean velocity of the perturber relative to the radiating atom and N is the number density of perturbers. From this equation we obtain

$$\lim_{h \rightarrow 0} \frac{|\Delta \nu_m|}{\Delta \nu_{1/2}} = \frac{1}{2} \tan \frac{\pi}{p-1}. \quad (3)$$

The empirical formula (1) and the experimental

half-widths give $p=6$ for In/Argon. Then Eq. (2) yields the expressions for line shift and half-width which when expressed in units of wave number are:

$$\begin{aligned} \Delta \nu_m = & -4.18 \times 10^8 v R_0^2 (\text{r.d.}) \\ & - 2.04 \times 10^{28} v R_0^5 (\text{r.d.})^2 - O((\text{r.d.})^4) \quad \text{and} \quad (4) \\ \Delta \nu_{1/2} = & 1.145 \times 10^9 v R_0^2 (\text{r.d.}) + O((\text{r.d.})^3), \end{aligned}$$

with v and R_0 in cgs units. Equation (4) indicates that, for a constant temperature, the shift *vs* r.d. is *nonlinear*, while the half-width *vs* r.d. is linear as observed in the present case and also in many other cases.¹ By comparing Eqs. (1) and (4), one obtains

$$\begin{aligned} R_0 &= 7.5 \text{ \AA}, v = 1.9 \times 10^5 \text{ cm/sec for In4511/Argon,} \\ R_0 &= 8.4 \text{ \AA}, v = 1.4 \times 10^5 \text{ cm/sec for In4101/Argon.} \end{aligned} \quad (5)$$

Here, the difference in v between the two spectral lines is caused partly by temperature differences. The temperature used predicts that $v = 10^5$ cm/sec.

The line contours can be plotted according to Eq. (2), using these values (5) as parameters. This method of plotting the line contour is designated as Method I.

Further, Eq. (4) leads to

$$\begin{aligned} h &= -0.551[2.74(\Delta\nu_m/\Delta\nu_{1/2}) + 1], \\ R_0/v &= -2.35 \times 10^{-11}(1/\Delta\nu_{1/2})[2.74(\Delta\nu_m/\Delta\nu_{1/2}) + 1]. \end{aligned} \quad (6)$$

Hence the parameters h and R_0/v can be evaluated for each experimental line contour separately so as to be as self consistent as possible. In this way, another theoretical distribution can be obtained (Method II).

A comparison of experimental line shapes with those obtained from Methods I and II are given in Figs. 8 (a), (b), (c), (d), and (e). For the main part of the lines, the agreement is reasonably good within the experimental error.

One of the assumptions made in the derivation of Eq. (2) is that the collisions are adiabatic. Though the lower state $^2P_{3/2}$ associated with the line $\lambda 4511$ is known to split itself at a close encounter with a perturber, this agreement between the experimental and theoretical contours indicates that this effect on the broadening is small, at least for the major part of the line contours observed. The pressure effect arises mainly from the difference of the interactions for upper and lower states of the line. The present data implies that this difference is appreciably larger than the splitting of the substates at important distances between the perturbers and radiating atoms. This is also indicated by the difference of the half-widths of the two lines observed.

The broadening of the $^2P_{1/2}$ component ($\lambda 4101$) is larger because the difference of the interaction, averaged over substates, of an indium atom in the lower levels, $^2P_{1/2}$ and $^2S_{1/2}$ with an argon atom is larger than that in the $^2P_{3/2}$ and $^2S_{1/2}$ states. From values in Eq. (5) one obtains:

$$\begin{aligned} \gamma(\text{In4101/Argon}) &= 5.9 \times 10^{-31} \text{ cm}^6/\text{sec}, \\ \gamma(\text{In4511/Argon}) &= 4.6 \times 10^{-31} \text{ cm}^6/\text{sec}. \end{aligned}$$

B. Pressure Effects of Helium on In4101 and In4511

The analysis of observed pressure effects produced by light gases has not been developed in a quantitative manner because the theoretical assumptions are some-

what open to question. However, it may be of interest to see how it turns out as shown in the following Section.

The long tails of the violet wings for both lines broadened by He would be expected to appear due to the same cause as in In/Argon, although for each line the satellite band and the main line will smear together because the line itself may have a violet asymmetry. For alkali resonance lines, with helium atoms as perturbers, the optical collision diameter happens to be nearly the same order of magnitude as the sum of the atomic diameter of helium (3.5 \AA) and the absorbing atom. Probably In/He is a similar example and we expect that the effective optical collisions are taking place at shorter distances and that the important force is repulsive. The large adiabatic exchange splitting of the $^2P_{3/2}$ state at these distances might invalidate an extension of Eq. (2) to In/He because of nonadiabatic effects.

We are making an assumption that we have taken some average of the interactions for substates of the $^2P_{3/2}$ state. Thus the extension of Eq. (2) for the main part of the line shape may be used without serious error. This effective frequency interaction is again assumed to be of the type γ/r^p .

The asymmetry is given from Eq. (2) as

$$1 + 7.07 \times 10^{19} R_0^3 (\text{r.d.}) + 2.50 \times 10^{39} R_0^6 (\text{r.d.})^2 - 5.89 \times 10^{58} (\text{r.d.})^3 \quad (7)$$

for an attractive interaction. Since p cancels, Eq. (7) holds for any value of p . For a repulsive interaction, the asymmetry measured has to be inverted to be compared with Eq. (7). Though an experimental error involved in the asymmetry measurement is usually large, in the present case of In/He it will be the best to compare Eq. (7) with the experimental asymmetry to evaluate R_0 . It turns out that

$$R_0(\text{In4511/He}) = 4.9 \text{ \AA}, \quad R_0(\text{In4101/He}) = 4.8 \text{ \AA}. \quad (8)$$

To obtain the other parameter v we use the half-width since it is linear against r.d. The value of p obtained from Eq. (3) is 8.32 and 8.84 for $\lambda 4511$ and $\lambda 4101$, respectively. Then an extension of Eq. (2) for a repulsive interaction yields

$$\begin{aligned} \Delta\nu_{1/2}(\text{In4511/He}) &= 1.012 \times 10^9 v R_0^2 (\text{r.d.}), \\ \Delta\nu_{1/2}(\text{In4101/He}) &= 9.97 \times 10^8 v R_0^2 (\text{r.d.}). \end{aligned} \quad (9)$$

Thus, the experimental half-widths give

$$\begin{aligned} v(\text{In4511/He}) &= 4.8 \times 10^5 \text{ cm/sec}, \\ v(\text{In4101/He}) &= 4.9 \times 10^5 \text{ cm/sec}. \end{aligned} \quad (10)$$

The temperatures used for the observation of these two lines were very nearly the same ($\sim 900^\circ\text{C}$). It is interesting to note that if we calculate the velocity from that obtained for In4101/Argon (at 800°C) by using the

mass relationship, it was found that $v = 4.4 \times 10^5$ Mc/sec for helium, which is in good agreement with Eq. (10).

Using the values (9) and (10) for R_0 and v , respectively, an extension of Eq. (2) gives the formula for shift⁵:

$$\begin{aligned}\Delta\nu_m(\text{In4511/He}) &= 0.27(\text{r.d.}) + 2.5 \times 10^{-3}(\text{r.d.})^2, \\ \Delta\nu_m(\text{In4101/He}) &= 0.24(\text{r.d.}) + 2.3 \times 10^{-3}(\text{r.d.})^2.\end{aligned}\quad (11)$$

The force constants are easily obtained from $\gamma = vR_0^{p-1}$.

$$\begin{aligned}\gamma(\text{In4511/He}) &= 1.5 \times 10^{-48} \text{ cm}^{8.32}/\text{sec}, \\ \gamma(\text{In4101/He}) &= 2.1 \times 10^{-52} \text{ cm}^{8.84}/\text{sec}.\end{aligned}$$

With the values of R_0 , p and v a comparison between the experimental and theoretical line shapes can be readily made. Only Method I is used in this case because the position of the unshifted line modifies the small shift of In/He to a large extent percentagewise. The result as given in Fig. 8 (e) is in very good agreement.

C. The Satellite Bands

The observed violet satellite bands appearing close to both lines when perturbed by argon are probably

⁵ To compare Eq. (11) with experimental shifts, 0.78 cm^{-1} for $\lambda 4511$ and 0.54 cm^{-1} for $\lambda 4101$ have to be subtracted from Eq. (11). These values would originate in the obscure knowledge about the positions of unshifted lines.

due to the appreciable deviation in the potential at small impact parameters from the above van der Waals' type instead of due to molecular formation. For the satellite bands the statistical theory may be used since $\Delta\omega R_0/v \gg 1$. The adiabatic splitting of the potential curve for different substates at small impact parameters would be very large.⁶ The repulsive part of the potential is associated with the exchange effect due to the overlapping of the wave functions of the two atoms. Since an atom in the $^2P_{3/2}$, $|m| = \frac{3}{2}$ state has less electronic charge in the direction to the perturber than that in the $^2P_{3/2}$, $|m| = \frac{1}{2}$ state, the atom in the former state is subject to a smaller repulsion by the rare gas atom. Thus, if one constructs the potential curves for the two 2P states for various impact parameters, the curve for the $|m| = \frac{1}{2}$ substate of $^2P_{3/2}$ should split from that for the $|m| = \frac{3}{2}$ substate and should run outward.

The curve for the $|m| = \frac{3}{2}$ state of $^2P_{3/2}$ and that for $|m| = \frac{1}{2}$ of $^2P_{1/2}$ will have nearly the same shape. If these two substates are responsible for the violet satellites and if the intensity distribution of the entire lines is normalized, both satellites should have nearly the same shape but with a stronger intensity for the satellites associated with the $\lambda 4101$ ($^2P_{1/2}$) component, as observed. Transitions from the $|m| = \frac{1}{2}$, $^2P_{3/2}$ substate at these impact parameters contributes rather uniformly to the whole shape of the main line.

⁶ Private communication from H. Margenau.